Photochemistry on the Space Station—Aptamer Resistance to Space Conditions: Particles Exposure from Irradiation Facilities and Real Exposure Outside the International Space Station

Gaëlle Coussot,[1] Aurélie Le Postollec,[2] Sébastien Incerti,[3] Mickaël Baqué,[4] Clément Faye,[5]
Odile Vandenabeele-Trambouze,[6] Hervé Cottin,[7] Corinne Ravelet,[8] Eric Peyrin,[8] Emmanuelle Fiore,[8]
Flavie Vigier,* Jérôme Caron,[9] Didier Chaput,[10] Bartos Przybyla,[11] Thomas Berger,[11] and Michel Dobrijevic[2]

Abstract

Some microarray-based instruments that use bioaffinity receptors such as antibodies or aptamers are under development to detect signatures of past or present life on planetary bodies. Studying the resistance of such instruments against space constraints and cosmic rays in particular is a prerequisite. We used several ground-based facilities to study the resistance of aptamers to various types of particles (protons, electrons, neutrons, and carbon ions) at different energies and fluences. We also tested the resistance of aptamers during the EXPOSE-R2 mission outside the International Space Station (ISS). The accumulated dose measured after the 588 days of this mission (220 mGy) corresponds to the accumulated dose that can be expected during a mission to Mars. We found that the recognition ability of fluorescently labeled aptamers was not significantly affected during short-term exposure experiments taking into account only one type of radiation at a time. However, we demonstrated that the same fluorescent dye was significantly affected by temperature variations (−21°C to +58°C) and storage throughout the entirety of the ISS experiment (60% of signal loss). This induced a large variability of aptamer signal in our analysis. However, we found that >50% of aptamers were still functional after the whole EXPOSE-R2 mission. We conclude that aptamer-based instruments are well suited for *in situ* analysis on planetary bodies, but the detection step requires additional investigations. Key Words: Astrobiology—Cosmic rays—Biochip—Aptamers. Astrobiology 19, 1063–1074.

1. Introduction

IN THE CONTEXT of planetary exploration, space agencies call for the development of miniaturized techniques to search for traces of extant or extinct life. In particular, the use of instruments based on bioaffinity receptors, such as anti-bodies or aptamers, might be very efficient. In this technology, bioaffinity receptors are fixed to a solid surface to specifically capture their target. A signal is displayed when receptor–target recognition events occur.

Antibody-based biochips have been extensively studied in proteomic and functional genomics, and their scope has

[1]Institut des Biomolécules Max Mousseron (IBMM), Université de Montpellier, CNRS, ENSCM, Montpellier, France.
[2]Laboratoire d'Astrophysique de Bordeaux (LAB), Université de Bordeaux, CNRS, B18N, Pessac, France.
[3]Centre d'Etudes Nucléaires de Bordeaux Gradignan (CENBG), UMR 5797, Université de Bordeaux, Gradignan, France.
[4]German Aerospace Center (DLR), Institute of Planetary Research, Management and Infrastructure, Research Group Astrobiological Laboratories, Berlin, Germany.
[5]Cap Alpha, Colcom, Clapiers, France.
[6]IUEM—UMR 6197, Laboratoire de Microbiologie des Environnements Extrêmes (LMEE), Université de Bretagne Occidentale (UBO), Plouzané, France.
[7]Laboratoire Interuniversitaire des Systèmes Atmosphériques (LISA), UMR 7583, Université Paris Est Créteil et Université Paris Diderot, Institut Pierre Simon Laplace, Créteil, France.
[8]Département de Pharmacochimie Moléculaire, UMR 5063, Université Grenoble Alpes, CNRS, St. Martin d'Hères, France.
[9]Département de Radiothérapie, Institut Bergonié, Comprehensive Cancer Center, Bordeaux, France.
[10]DCT/ME/EM, Centre National d'Etudes Spatiales, Toulouse, France.
[11]German Aerospace Center, Institute of Aerospace Medicine, Cologne, Germany.
*This coauthor is now working for private companies.

been extended to the field of astrobiology. Indeed, due to the benefits of high throughput and miniaturization, and small volume consumption, antibody-based biochips have been proposed to detect biomarkers, especially organic ones, in the search for extraterrestrial life (Parro *et al.*, 2005, 2008, 2011a; Le Postollec *et al.*, 2007; Martins, 2011; Sims *et al.*, 2012; McKay *et al.*, 2013; Smith and Parro, 2014).

Space is a hazardous environment, with high fluxes of ionizing radiation, from primary particles of galactic cosmic radiation (GCR) and solar energetic particles (SEPs), to secondary particles produced by the interaction of primary particles with environment materials. One main concern relies on the resistance of biochips to the cumulative effects of these types of radiation. In recent years, studies have been performed to evaluate the resistance of antibody reagents to space constraints, especially regarding the effect of specific particles on antibody-binding performances (Le Postollec *et al.*, 2009a, 2009b; Baqué *et al.*, 2011a, 2017; de Diego-Castilla *et al.*, 2011; Coussot *et al.*, 2017).

To complement ground-based radiation studies, a short-term mission was performed on the BIOPAN-6 low-Earth orbit platform to demonstrate the effects of cumulative radiation on the antibodies' ability to bind to their respective antigens (Derveni *et al.*, 2012, 2013). For the absorbed radiation doses during the 12 days of exposure, the freeze-dried antibodies packaged into laser-cut glass fiber pads were unaffected with regard to their recognition performances in the condition of the experiment. Furthermore, in the frame of the Biochip for Organic Matter Analysis in Space (BiOMAS) project and part of the Photochemistry on the Space Station (PSS) experiment, biochip models, in which antibodies were immobilized onto a surface, have been installed outside the International Space Station (ISS) on the EXPOSE-R2 platform, for a real long-term exposure (>18 months) to spatial constraints (Vigier *et al.*, 2013; Cottin *et al.*, 2015, 2017).

Our recent results show that our biochip models resist to an 18-month extravehicular mission (Coussot *et al.*, 2019). This work, in combination with the ground-based radiation studies, permits us to assess the antibodies' ability to bind to their respective antigens even after a long-term exposure to the real space environment. These experiments indicated that antibody-based instruments seem well suited for the search for organic matter in *in situ* planetary bodies' samples.

Other target-binding reagents with specificity and binding affinity rivaling with those of antibodies are aptamers. Aptamers are short, single-stranded nucleic acids, able to bind from small molecular weight molecules up to proteins. Aptamers have demonstrated some interesting advantages over antibodies: production at low cost, specificity against small and nonimmunogenic molecules, thermal stability, and ability to maintain their structures over repeated cycles of denaturation/renaturation (Song *et al.*, 2012). From diagnostics to food safety or therapeutics, aptamers have shown their interests in arrays and biosensors development (Song *et al.*, 2012; Dong *et al.*, 2014; Gotrik *et al.*, 2016; Rozenblum *et al.*, 2016).

The first investigation on the ability of nucleic acid aptamers to maintain their binding performances under simulated cosmic radiation, in particular 2 MeV proton effects, was carried out by Baqué *et al.* (2011b). The results revealed that, under the protons flux and energy tested, there were no deleterious effects on the binding affinity of the irradiated DNA aptamer. So far, no more investigations on the effect of high-energy particles on aptamer performances have been reported.

In this study, we first present a set of experiments carried out these last 7 years in ground-based particles accelerator facilities to study the effect of different types of incident particles (protons, electrons, neutrons, and carbon ions) at different energies and fluences, on the ability of a model aptamer to recognize its target. The second part of the article discusses the results obtained after a long time exposure to real space constraints of aptamer samples in the framework of the PSS project (Cottin *et al.*, 2015).

2. Materials and Methods

2.1. Chemicals, reagents, and materials

L-tyrosinamide (*L*-Tym), fluorescein dye (F), sodium bicarbonate (NaHCO$_3$, ≥99.5%), sodium carbonate (Na$_2$CO$_3$, ≥99.5%), and Tris(hydroxymethyl) aminomethane (Tris ≥99.8%) were purchased from Sigma-Aldrich (Saint-Quentin Fallavier, France). NaCl and MgCl$_2$ of analytical grade were obtained from Chimie-Plus Laboratoires (Bruyères de Pouilly, France) and Panreac Quimica (Barcelona, Spain), respectively. The aptamer anti-*L*-Tym containing 49 nucleotides and modified in its 3′ end by fluorescein (no. 4551724; MW 15860.5 g/mol) was provided by Eurogentec (Angers, France). This aptamer was chosen as an aptamer model; it has been reported as 49merYm3′F in the text, and had the following sequence: 5′-AATTCGCTAGCTGGAGCTTGGATTGATGTGGTGTGT GAGTGCGGTGCCC-F-3′ (four different batches were used: batch 1 for ground-based neutrons, electrons, and protons experiments; batch 2 for ground-based ^{12}C experiments; batch 3 for ISS mission; and batch 4 for postflight experiments). The ultrapure water (18.2 MΩ) was obtained from a Purite Still Plus water purification system (Thame, United Kingdom). Other chemicals are of analytical grade and used as received. Nunc MaxiSorp™ polystyrene 96-well plates were obtained from VWR (France), and were used as sample containers during the freeze-drying step and throughout the laboratory radiation exposures. In case of ISS experiment, Corning DNA Bind™ 8-well strip plate with N-hydroxysuccinimide modified surface (NHS-wells) was provided by Sigma-Aldrich (Saint-Quentin Fallavier). NHS-wells were manufactured by Air Liquide (Sassenage, France) to fit perfectly with the shape and size of EXPOSE-R2 closed cells provided by the French Space Agency (CNES, Toulouse) (Vigier *et al.*, 2013). The home-designed NHS-wells had a diameter of 8.4 mm with a 7.1 mm height. Teflon caps were specially manufactured by Air Liquide to close the well (Fig. 1a).

2.2. Freeze drying and sample preparation

Particle irradiation effects were evaluated on both freeze-dried 49merYm3′F aptamer and fluorescein dye. One hundred microliters of 49merYm3′F aptamer or fluorescein solution at 500 n*M* in ultrapure water (dilution by 1/40 from a stock solution freshly prepared at 20 μ*M* from aptamer commercial vial) were put into MaxiSorp wells (commercial or home-designed well format), and freeze-dried according to a protocol optimized for the freeze drying of small volume of reactants (Coussot *et al.*, 2018). In brief, MaxiSorp wells were put into a homemade
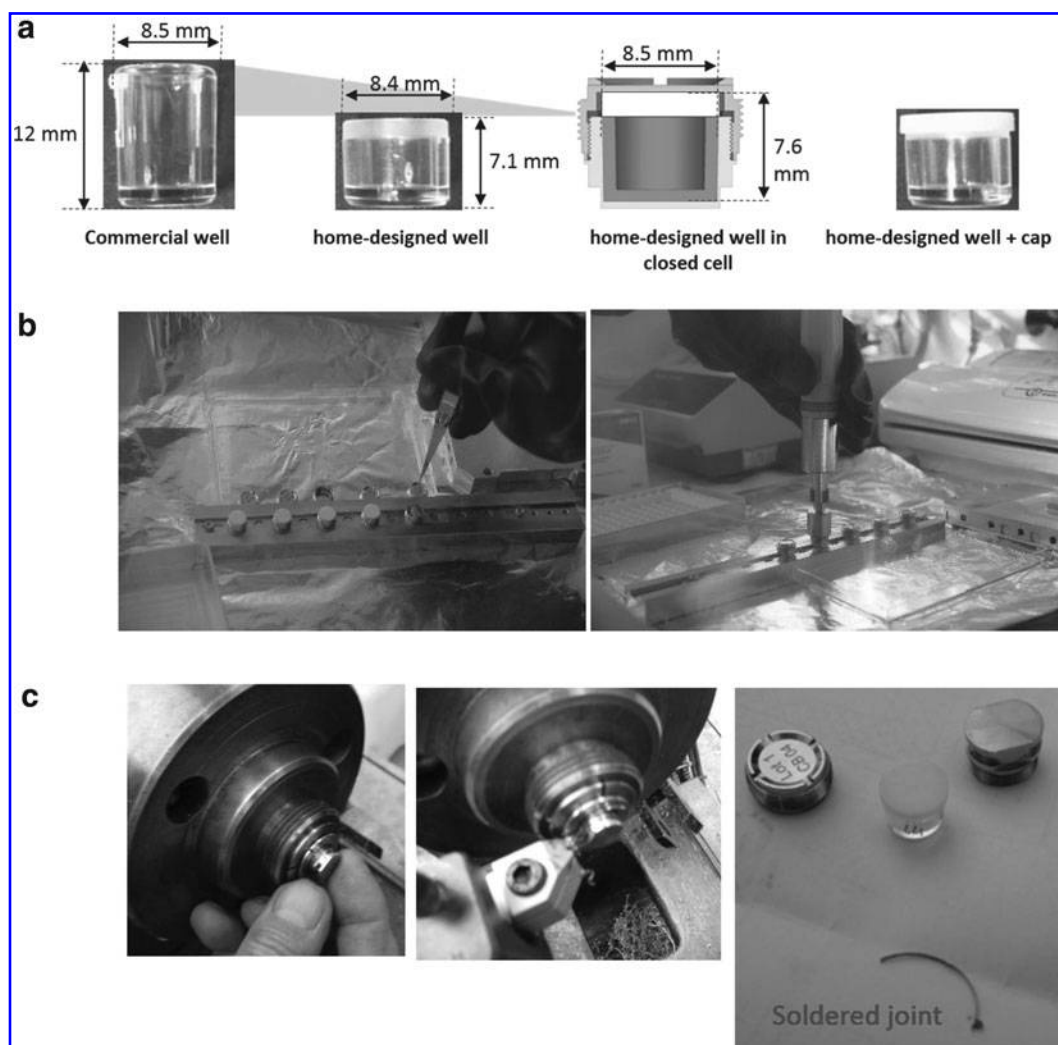
FIG. 1. (a) Design and dimension of the home-designed well and its cap. (b) Incorporation of capped well into CNES cells under controlled atmosphere and final screwing of closed CNES cells using a torque screwdriver. (c) Postflight opening of the CNES cells to remove the soldered joint.

aluminum holder, and liquid nitrogen was added to freeze the samples. The aluminum holder was then placed into the central part of a freeze dryer with a top-press device (Christ Alpha 2–4 from Martin Christ GmbH, Germany). Freeze drying was performed overnight (condenser temperature −85°C, vacuum 0.05 mbar). The chamber of the freeze dryer was filled with nitrogen gas before closing the sample-containing aluminum holder, which kept sealed hermetically the samples and sheltered them from the moisture and light until its opening. The opening of the aluminum holder was done in a glove box under a controlled atmosphere of helium (10% He) in argon (Ar) provided by Air Liquide (Sassenage) to maintain a relative humidity (RH) level of 10–15%. During our experiments, the RH and air temperature were controlled with a thermohygrometer Testo 605-H1 (Testo, France). RH was 12% ± 3%, and air temperature was 22.8°C ± 2.3°C. After opening the aluminum holder, freeze-dried samples were sealed within a plastic bag by using a vacuum sealing device FoodSaver™ (Fischer Scientific, France) and stored at 4°C in the dark until running laboratory irradiation experiments.

In case of ISS experiments, 150 μL of carbonate buffer (pH 9.4, 0.1 *M*) was added to the home-designed NHS-wells to deactivate reactive sites. The incubation took place overnight at room temperature. After successive water washings, 100 μL of 49merYm3′F aptamer/fluorescein solution at 500 n*M*, freshly prepared in ultrapure water, was pipetted into each well. The freeze-drying procedure was run as described above. After opening the aluminum holder in the above controlled atmosphere, freeze-dried samples were capped and directly transferred into the CNES closed cells with a tool vacuum suction pen (FFQ939 from Mayf's Online Shop, China). The CNES closed cells were then screwed with a final tightening of 0.7 Nm with a torque screwdriver TorqueVario®-S (Wiha, Germany) (Fig. 1b) (Vigier *et al.*, 2013). Soldering of the CNES cells and their integration to the sample carriers were done according to CNES internal procedures.

2.3. Experiments on ground-based particles accelerator facilities

The composition of cosmic rays is dominated by protons, electrons, alpha particles, and a small fraction of heavy ions (such as carbon, oxygen, and up to iron ions). Interactions of

these primary particles with matter produce secondary particles such as electrons and neutrons. So, experiments on ground-based facilities (producing protons, electrons, neutrons, and carbon ions) have been performed to study the impact of GCR and SEPs on the affinity of the 49merYm3′F aptamer toward its *L*-Tym target. The set of experimental conditions is summarized in Table 1, and detailed in the work of Baqué *et al.* (2017). These are considered as short-term exposure experiments taking into account only one type of radiation at a time to study the potential effects on the 49merYm3′F aptamer-*L*-Tym bindings. All experiments were repeated at least three times per irradiation condition to have three titration curves per analytical condition. Six replicates were prepared for fluorescein dye. Freeze-dried samples were irradiated directly in their sealed bags. The influence of the bag during irradiation experiments was simulated with Geant4 Monte Carlo toolkit and demonstrated to be negligible (Baqué *et al.*, 2017). Controls are the reference samples that have been freshly prepared the day of analysis: they did not undergo freeze-drying process, neither transportation nor storage at 4°C. We previously verified that freeze drying does not induce any effects on binding curves nor in K_d value. So, controls (freshly prepared references) can be used in place of lyophilized-nonirradiated samples for ground-based experiment interpretations. Analyses were performed using fluorescence polarization (FP) assay for aptamers as described in Section 2.7, and in direct fluorescence for fluorescein dyes as described in Section 2.6.

2.4. Experiment outside the ISS

Simulating radiation environment in Earth facilities is highly complicated, since it is almost impossible to include all constraints encountered during an entire space mission all together (long duration storage, transportation, takeoff/landing shocks, thermal constraints, and cumulative effects of cosmic ray particles). For that purpose, 11 samples (7 ground controls, 4 exposed samples also denoted as ISS samples) took part in the "Biochip in PSS experiment" (Vigier *et al.*, 2013; Cottin *et al.*, 2015) during the EXPOSE-R2 mission. These samples were simultaneously prepared, within the same freeze-drying batch, as that described in Section 2.2. The four exposed CNES cells were spread on the two exposure levels of the Tray 3 of the EXPOSE carrier dedicated to the PSS experiment. Disposition of the two CNES cells on the sample carrier was the

same for the upper and the lower level of the sample carrier. Launch to ISS (July 23, 2014) and storage inside ISS were at ambient temperature (22–25°C on average) (Rabbow *et al.*, 2017). Then, EXPOSE-R2 platform was placed outside the ISS on the Universal platform D on August 18 with opening of the valves on August 20, and removal of the UV shield on October 22, 2014. On February 3, 2016, trays were covered and brought back inside the ISS. Thus, the exposed samples spent 566 days outside the ISS over the 588 days of the mission (1 year, 8 months).

Into each CNES cell, two thermoluminescent detectors (TLDs) were placed at the bottom of the cell, below the samples. These passive dosimeters were analyzed at the end of the mission (for detailed methods of analysis, see Berger *et al.*, 2012, 2015), and revealed that the absorbed dose by our aptamer samples was ∼220 mGy for the 588 days of the mission. This absorbed dose is consistent with doses expected for a mission to Mars. Indeed, considering Geant4 simulations in the work of Le Postollec *et al.* (2009b), this absorbed dose (220 mGy) corresponds to 8 months travel and 6 months at Mars surface. Considering doses measured by Curiosity rover (Hassler *et al.*, 2014), this dose corresponds to a mission to Mars with 8 months travel and 18 months at the surface.

During their extravehicular exposition, the samples on Tray 3 were submitted to temperatures varying between −20.9°C and 57.98°C (Rabbow *et al.*, 2017). Accurate measurements of the CNES exposed cells temperature were provided by the temperature control interface of the Planetary and Space Simulation Facilities (Microgravity User Support Center [MUSC], www.musc.dlr.de/expose-r-2/; Fig. 2a). On March 2, 2016, EXPOSE-R2 Tray 3 landed on Earth. During transit from Baïkonur cosmodrome to Moscow and from Moscow to German Aerospace Center (DLR, Germany), a recording of temperatures was done; the temperatures oscillated between 20°C and 24°C. Then from DLR to Laboratoire Interuniversitaire des Systèmes Atmosphériques (LISA, Paris Est-Créteil) (Rabbow *et al.*, 2017) and Paris to Montpellier, a controlled chamber at 4°C was used during transportation in the summer period. Deintegration of the exposed CNES cells from the sample carriers was done according to MUSC/DLR/ESA/CNES internal procedures. On June 24, 2016, the soldered joint of all the CNES cells (including ground references) was removed by using a mechanical lathe and a manufactured CNES tool, in the mechanics department of the Montpellier University

TABLE 1. MAIN EXPERIMENTAL CONDITIONS FOR NEUTRON, PROTON, ELECTRON AND CARBON IONS IRRADIATIONS

Date	Place		Particule type	Fluence (particles/cm²)	Energy	Irradiation duration
April 27, 2012	Istituto Nazionale di Fisica Nucleare	Catania, Italy	^{12}C	$F_c = 2.10^6$	$E_c = 62$ MeV/nuc	$D_c = 7$ min
July 7, 2011	Institut Bergonié	Bordeaux, France	Electrons	$F_{e1} = 3.10^{11}$ $F_{e2} = 3.10^{10}$	$E_e = 9$ MeV	$D_{e1} = 70$ min $D_{e2} = 7$ min
June 1, 2010	Centre de Recherche du Cyclotron	Louvain-la-Neuve, Belgium	Neutrons	$F_{n1} = 3.10^{13}$ $F_{n2} = 3.10^{12}$	$E_n = 17$ MeV (mean)	$D_n = 22$ min
March 6, 2010			Protons	$F_{p1} = 3.10^{12}$ $F_{p2} = 3.10^{11}$	$E_{p1} = 25$ MeV $E_{p2} = 50$ MeV	$D_{p1} = 1$ h 40 min $D_{p2} = 10$ min

Subscript letters indicate the particle type and subscript numbers are used to differentiate the applied conditions. Units for fluences are in particles per cm². Technical details have already been reported in Baqué *et al.* studies (Baqué *et al.*, 2017).
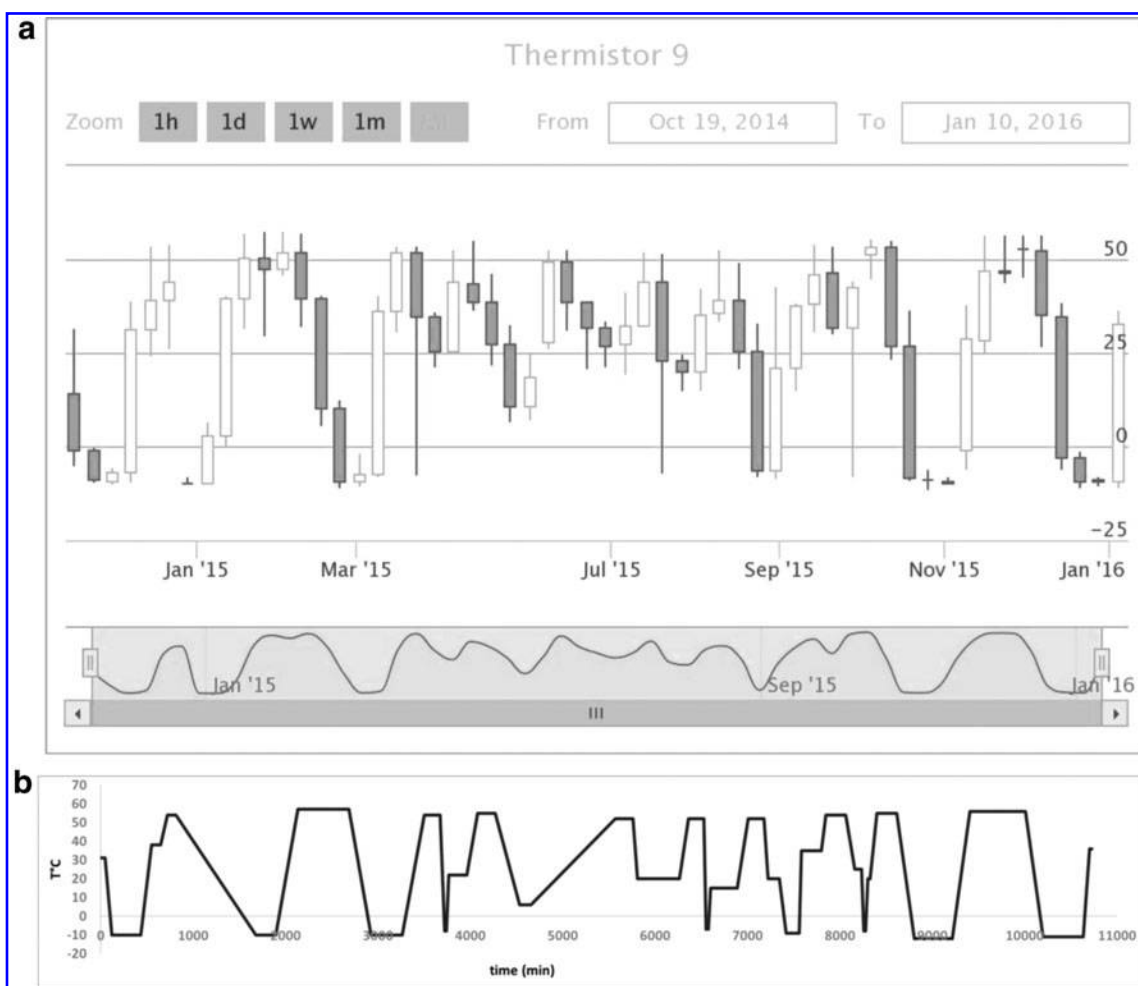
FIG. 2. **(a)** Overview of the EXPOSE-R2 temperature profiles for Tray 3 on thermistor 9 sensor during the EXPOSE-R2 mission (from October 19, 2014 to January 10, 2016, www.musc.dlr.de/expose-r-2/). **(b)** Ground thermal cycling experiments mimicking thermal CNES cells exposure outside the ISS but in accelerated time: 1 h of EXPOSE-R2 mission was converted into 1 min to carry out this experiment in laboratory, and temperature amplitude was similar (referred to as long cycle in the text). ISS, International Space Station.

(Fig. 1c). Samples were immediately sealed in a FoodSaver bag (Fischer Scientific) and stored in the dark at 4°C until analysis with FP assays.

2.5. EXPOSE-R2 mission ground references

During the same period, experiments have been performed on ground to control the long-term behavior of the 49merYm3′F aptamer upon storage but not exposed to space constraints. Two ground CNES cells were stored at the French Space Agency (CNES) by maintaining an accurate temperature control at 3.9°C ± 0.8°C over that period. These samples were named as "CNES 5°C" samples. Three ground CNES cells were kept in DLR (Cologne, Germany): two ground CNES cells were stored at 5°C ("DLR 5°C" samples) and one ground CNES cell underwent the same thermal history as ISS samples ("DLR ΔT" sample) (Fig. 2a). In addition, the behavior of two additional ground samples was studied at DLR combining long time storage, varying thermal environment as ISS ones, and UV radiation ("DLR ΔT+UV" samples) (Rabbow *et al.*, 2017). Calibrated Bentham 150 double monochromators instrument equipped with a SOL2000 lamp (Dr. K. Hönle GmbH, Martinsried, Germany) was used

to provide a spectrum similar to that of sunlight. All of these seven ground CNES cells were brought back to Montpellier to be handled simultaneously with the exposed CNES cells during all the desoldering process and 4°C storage (Section 2.4) before running FP assays (Section 2.7). However, data of DLR ΔT and DLR ΔT+UV samples have not been added to our analysis due to the lack of precision of the applied temperatures.

2.6. Additional ground thermal cycling experiments

The 49merYm3′F aptamer and fluorescein dye were freeze-dried at 500 nM in ultrapure water as described in Section 2.2. Thermal cycling experiments were carried out on freeze-dried samples in their sealed bags in a temperature test chamber (Vötsch VT 4004). Two independent thermal variation experiments were performed: one with a sharp rise in temperature (5°C/min) until a 1 h plateau at 80°C (referred to as "80°C peak" in the text) and a long cycling period (178.8 h or 7.45 days) mimicking thermal variations of exposed cells (Fig. 2b) with an amplitude of ∼70°C (referred to as "long cycle" in the text). After reconstitution of freeze-dried product with 120 μL of deionized water,

100 μL was pipetted into black 96-well half-area microplates from Greiner Bio-One (Courtaboeuf, France) to measure fluorescence intensity (response) of the signal abbreviated as RFS. Fluorescence measurements were done on a Tecan's Infinite® F500 microplate reader (Mannedorf, Switzerland) having excitation and emission filters at 488 and 525 nm, respectively. A blank signal with neither aptamer nor fluorescein dye was used to evaluate noise value (abbreviated as RFN in the text). Results are presented as signal-to-noise (S/N) ratio equal to RFS/RFN.

2.7. Aptamer-based FP assay

For all experiments carried out in ground-based particles accelerator facilities and the overall ISS mission, a structure-switching aptamer assay based on a FP approach (Fig. 3) was used to evaluate the binding ability of the 49merYm3′F aptamer toward its L-Tym target. The approach, described by Ruta *et al.* (2009) and Perrier *et al.* (2010), is based on monitoring the fluorescence anisotropy change (Δr) of an aptamer labeled by a single fluorescent dye at its 3′ end. Fluorescence anisotropy change Δr was calculated as the difference between the measured anisotropy (r) of the labeled aptamer–target complex and the anisotropy in the absence of target (r_f), which was prepared by replacing the L-Tym target solution by deionized water. The optimized binding buffer for FP assay consisted of 10 mM Tris–HCl, pH 7.5, 10 mM MgCl$_2$ and 50 mM NaCl (Zhu *et al.*, 2011). The aptamer solutions (500 nM) were heated at 80°C for 5 min for denaturation, then left to stand at room temperature in the dark for 30 min. One hundred microliters of the renatured aptamer solutions were deposited into black 96-well half-area microplates containing the increasing concentrations of L-Tym (0.5/1/2.5/5/7.5/10 or 12.5/25.0/40.0 or 50.0/80.0/200.0 μM) for measurements on Tecan's Infinite M1000 PRO (Tecan, France). Excitation was set at 485 ± 20 nm, and emission was collected with 535 ± 25 nm bandpass filters.

2.8. Data interpretation and statistical analysis

For a 1:1 stoichiometry, the measured anisotropy (r) can be linked to the apparent dissociation constant K_d through the following relation:

$$r = \frac{r_f K_d + r_b c}{K_d + c}, \tag{1}$$

where r_f is the anisotropy in the absence of target, r_b is the anisotropy of maximally target-associated aptamer, and c is the concentration of free target. For a limiting aptamer probe concentration, the total concentration of target (c_T) in the reaction system approximates the free target concentration c. The nonlinear regression of the r versus c ($\approx c_T$) plots, where r_b and K_d constituted the adjustable parameters, was achieved by using the Table-Curve 2D software (Systat Software Gmbh, Erkrath, Germany).

To evaluate cosmic rays effects on freeze-dried exposed aptamers, control samples were prepared with an aptamer probe that did not undergo freeze-drying process or irradiation (reference sample). Binding affinity data for exposed samples and control samples were compared by using the relative dissociation constant value (relative K_d) expressed as follows:

$$\frac{K_{d\,(\text{irradiated})}}{K_{d\,(\text{control})}}. \tag{2}$$

Relative K_d values are reported in Table 2.

For the ISS experiments, relative K_d were estimated from freeze-dried ground samples stored at 5°C in DLR facility during all the duration of the mission. "Flight samples" corresponded to ISS samples that undergo all cumulative effects of the mission (flights, extravehicular exposure, and transportation). Relative K_d values are reported in Table 3.

All data are reported as mean ± the standard deviation from at least four replicate experiments. Statistical significance of the assays was determined by using the Student t test ($p = 0.05$).

3. Results

We first determined a reference value of the affinity of the aptamer used to its target. In the various FP assays we performed, the concentration of 49merYm3′F aptamer was
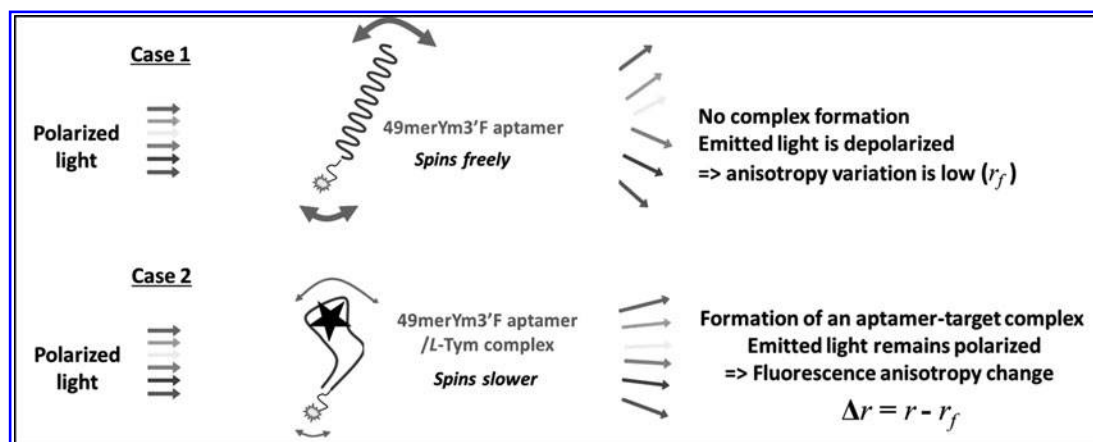

FIG. 3. Principle of the FP assays. A fluorescence anisotropy increase is observed upon the formation of a labeled aptamer–target complex. FP, fluorescence polarization.

TABLE 2. EXPERIMENTS ON GROUND-BASED PARTICLES
ACCELERATOR FACILITIES

*Experiments on ground-based particles accelerator
facilities*

Particle type	Relative K_d for irradiated samples (fluence, energy, duration, replicates)
^{12}C	1.01 ± 0.15 (F_c; E_c; D_c; 3)
Electrons	1.09 ± 0.22 (F_{e1}; E_e; D_{e1}; 4)
	0.99 ± 0.20 (F_{e2}; E_e; D_{e2}; 4)
Neutrons	1.19 ± 0.35 (F_{n1}; E_n; D_n; 3)
	0.99 ± 0.16 (F_{n2}; E_n; D_n; 3)
Protons	0.88 ± 0.21 (F_{p1}; E_{p1}; D_{p1}; 3)
	0.80 ± 0.15 (F_{p1}; E_{p2}; D_{p1}; 3)
	0.93 ± 0.18 (F_{p2}; E_{p1}; D_{p2}; 3)
	0.84 ± 0.16 (F_{p2}; E_{p2}; D_{p2}; 3)

Relative dissociation constant values (relative K_d) (Eq. 2) derived from the titration curves obtained for irradiated samples ($n = 3$ or 4) after ground-based irradiation experiments with at least ($n = 3$) reference samples.

constant (500 nM), and its target L-Tym increased in concentrations from 0.5 to 200 μM (10 levels of concentrations, see experimental part). Binding data of 49merYm3′F aptamer to L-Tym were globally fit to four parameter logistic regressions permitting the calculation of K_d (1.54 ± 0.14 μM, aptamer batches 1, 2, 3, $n = 14$), which is comparable with previously published data (Ruta *et al.*, 2009).

3.1. Irradiation effects on aptamers during ground-based experiments

To minimize experimental error, all assays were performed at least in triplicate. Affinity curves do not reveal significant differences in anisotropy change Δr (Fig. 4). The corresponding relative K_d values were calculated (Eq. 2) and reported in Table 2. The aim of this study, according to the particle types, fluences, energies, and exposure durations, is to determine whether irradiated samples undergo damaging effects on the aptamer leading to a decrease in its ability to bind to its target or leading to a decrease of the detection signal. Although no effect was detected with ^{12}C ions at high energy (Fig. 4a) (statistically identical K_d values), differences in Δr were observed with other particles. For instance, in

TABLE 3. BIOCHIP IN PSS EXPERIMENT
DURING THE EXPOSE-R2 MISSION

*Biochip in PSS experiment during the EXPOSE-R2
mission*

Sample type	Relative K_d (replicates)
Ground control (CNES 5°C)	0.82 ± 0.10 (2)
Ground control (DLR 5°C)	1.00 ± 0.10 (2)
Ground control (DLR ΔT)	1.29 ± 0.28 (1)
Ground control (DLR ΔT+UV)	0.93 ± 0.20 (2)
Flight (upper tray)	0.94 ± 0.14 (2)
Flight (lower tray)	1.07 ± 0.21 (2)

Relative dissociation constant values (relative K_d) (Eq. 2) derived from the titration curves issued from the "Biochip in PSS experiment" during the EXPOSE-R2 mission.

Fig. 4b, a slight difference was observed in Δr between the two irradiated samples with electrons. However, analysis of the relative K_d for both irradiated samples shows that they were statistically identical ($p > 0.05$) to the corresponding reference. This suggests that the recognition abilities of the 49merYm3′F aptamer were not affected by the irradiation process even when using higher fluence and irradiation duration. The same phenomenon was observed with neutrons: the higher fluence F_{n1} induced a larger decrease in anisotropy change Δr (Fig. 4c). The relative K_d value corresponding to irradiated sample with (F_{n1}; E_n; D_{n1}) radiation conditions (which presents higher variability) stayed statistically identical to the reference one. Consequently, we hypothesized that high fluences of electrons and neutrons might have deleterious effects on the fluorescein dye. To verify that point, we ran a Student t test on fluorescence intensities obtained for fluorescein dye before and after irradiations. It revealed that significant differences could be observed with up to 40% loss in fluorescence signal for high fluence F_{n1} for neutrons and fluence F_{p1} at both energies E_{p1} and E_{p2} for protons. So, potential degradation of fluorescein dye might occur with higher fluence. Thus, after exposure to (F_{e1}; E_e; D_{e1}) radiation with electrons beam and (F_{p1}; E_{p1}) and (F_{p1}; E_{p2}) radiation with protons beam, fluorescence anisotropy changes might not be due to alteration of binding but rather suggest some alterations of the fluorescein dye emitting properties. In addition, with protons, cumulative effects were observed. Indeed, the results of FP measurements after protons irradiation showed a small discrepancy between the reference sample and the four irradiated ones (Fig. 4d). Although K_d values were slightly smaller than those of the reference (Table 2), they remained statistically identical. All radiation configurations tested led to a similar anisotropy change Δr, which could suggest that there was no important damage in the structure of the 49merYm3′F aptamer that consequently could alter the binding to its target L-Tym. Compared with our previously published data (Baqué *et al.*, 2011b), showing that 2 MeV protons had no effect on the binding affinity of irradiated 49merYm3′F aptamer neither on the fluorescein dye, the present data might suggest that higher energies of protons (25/50 MeV) alter the fluorophore.

3.2. ISS experiments

Since radiation gradients were observed on the EXPOSE platform in previous ISS missions (Berger *et al.*, 2012, 2015), the four exposed aptamers "Flight samples" were spread on the two exposure levels of the Tray 3 of the EXPOSE carrier dedicated to the PSS experiment, but with the same disposition on the upper and lower levels of the sample carrier. However, measurements performed with passive dosimeters during the EXPOSE-R2 mission revealed, *a posteriori*, that the absorbed dose difference between cells at upper and lower levels was extremely low (~ 3 mGy for the whole mission corresponding to 1.4% of the total). Some TLDs stacks composed of 11 TLDs included into Tray 3 structure bring explanations on this very low difference. As can be seen in Fig. 5, absorbed dose decreases when shielding increases but after ~ 0.75 g/cm^2 of shielding, the absorbed dose measured remains quasi stable and the dose decrease evolves very slowly even if shielding

is significantly increased. As the estimated shielding of TLDs placed into cells on the upper level is $\sim 0.82 \, \text{g/cm}^2$, it explains the very low absorbed dose difference observed between both levels.

Calculated value of K_d from independently and freshly prepared reference samples was $1.58 \pm 0.12 \, \mu M$ (aptamer batch 4), which is comparable with the above reference

value $(1.54 \pm 0.14 \, \mu M)$. However, K_d values from the eight mission samples appeared to be on average 1.5–2 times higher. We previously verified that freeze drying induced no effects on binding curves nor in K_d value. However, storage stability analyses of freeze-dried 49merYm3′F aptamer (batches 1 and 2), carried out at 4°C for 20 days and 7 months, showed differences in anisotropy change Δr for the
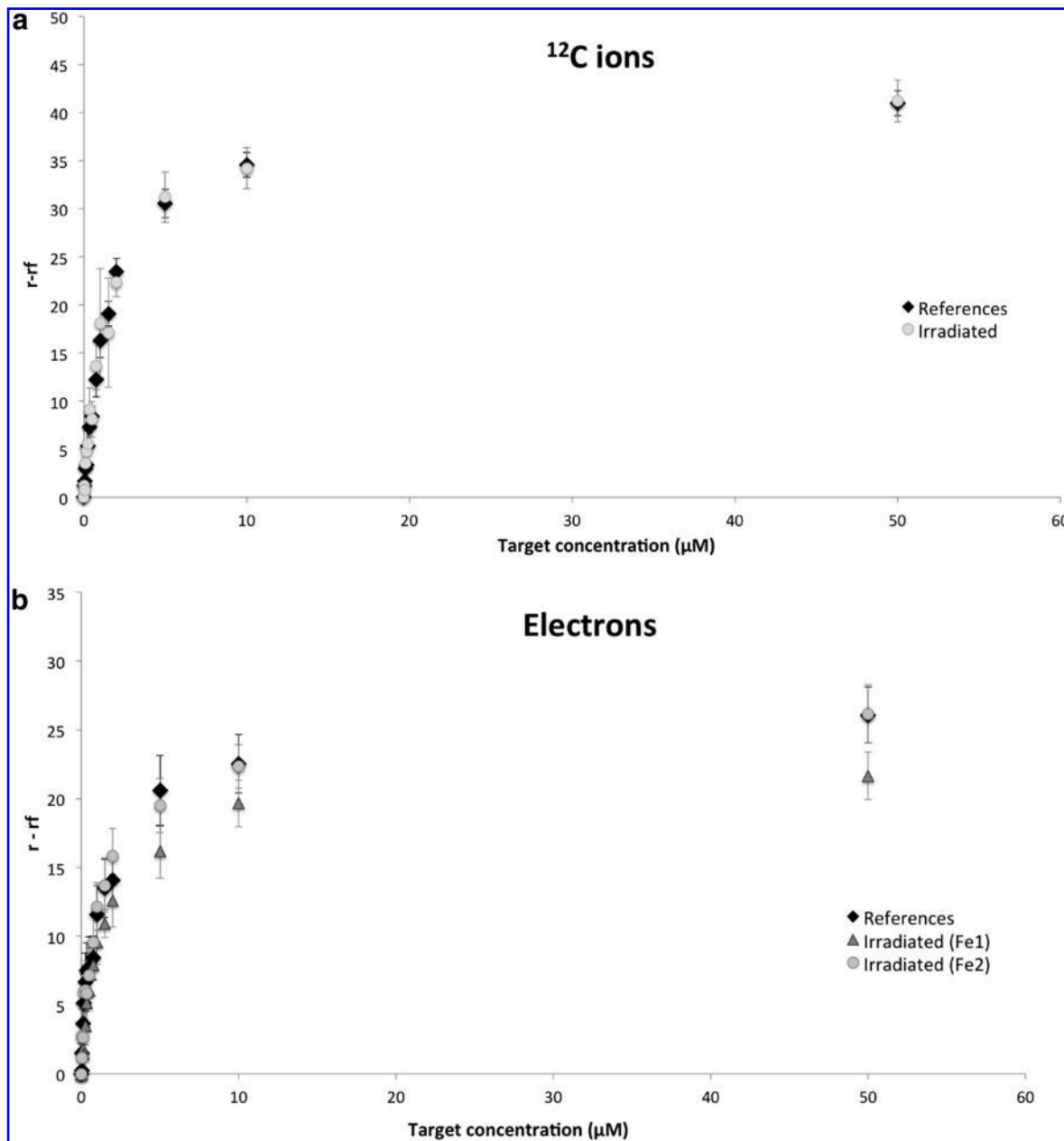

FIG. 4. Affinity curves for 49merYm3′F aptamer with additions of L-Tym obtained for reference (nonirradiated sample), and irradiated samples with particles at various fluence (F), energy (E), and irradiation duration (D), for details see Table 1. The saturation curves were used for the determination of dissociation constant values (K_d) (Eq. 2) by nonlinear regression analysis. The calculated relative K_d are listed in Table 2. Reference samples ($n = 3$ or 6) are labeled in black diamond. **(a)** Irradiated samples with ^{12}C ions (F_c; E_c; D_c) are illustrated in gray cycle ($n = 3$). **(b)** Irradiated samples are represented in dark gray triangle with electron fluences of 3.10^{11} p/cm^2 (F_{e1}; $n = 4$) and with a gray circle for 3.10^{10} p/cm^2 fluence (F_{e2}; $n = 4$). **(c)** Irradiated samples with neutron fluences of 3.10^{13} p/cm^2 (F_{n1}; $n = 3$) are illustrated in gray square and 3.10^{12} p/cm^2 (F_{n2}; $n = 3$) in empty circle. **(d)** Irradiated samples with protons fluence of 3.10^{12} p/cm^2 with energy of 25 MeV (F_{p1}; E_{p1}; $n = 3$) are represented in empty circle, and in gray circles for an energy of 50 MeV (F_{p1}; E_{p2}; $n = 3$). Fluences of 3.10^{11} p/cm^2 with energy of 25 MeV (F_{p2}; E_{p1}; $n = 3$) are plotted with an empty triangle, and with an energy of 50 MeV (F_{p2}; E_{p2}; $n = 3$) with a gray triangle.
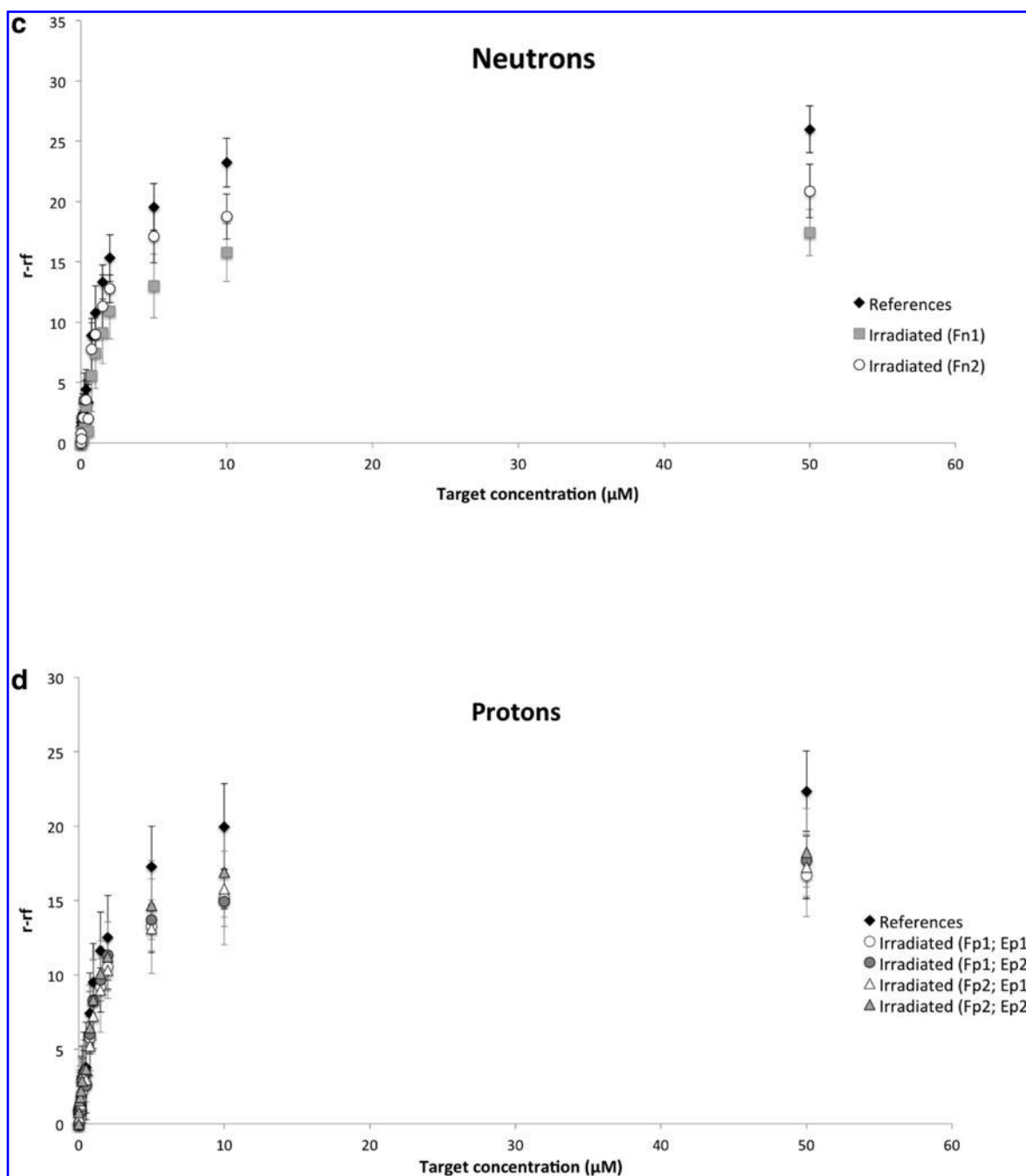
Figure 4c, d. (continued)

different storage times and aptamer batches (data not shown). Consequently, to only take into account the effects encountered during the ISS mission (flights, extravehicular exposure, and all transportations during the mission), relative K_d were calculated by using the freeze-dried ground samples stored at 5°C in DLR facility during all the duration of the mission. The binding curves and the corresponding relative K_d values are reported in Fig. 6 and Table 3, respectively. We distinguished two groups of affinity curves. Group 1 concerns the highest measured anisotropy change Δr with both ground controls stored at 5°C (DLR and CNES) during the mission. Group 2 represents the flight

samples. We note that the ''lower tray'' samples seem to have a different behavior than the flight samples exposed in the ''upper tray.''

Based on these observations, an effect due to the temperature variations during the mission can be invoked. To test this hypothesis, postflight ground thermal cycling experiments were carried out on the 49merYm3′F aptamer and the fluorescein dye over a 80°C short peak of temperature and a long cycle mimicking thermal variations of flight samples (see Section 2.6 of the experimental part and Fig. 2b). S/Ref values were 74.5 ± 15.1, 62.1 ± 23.5, and 59.0 ± 14.9 for the freeze-dried fluorescein reference, the 80°C peak, and
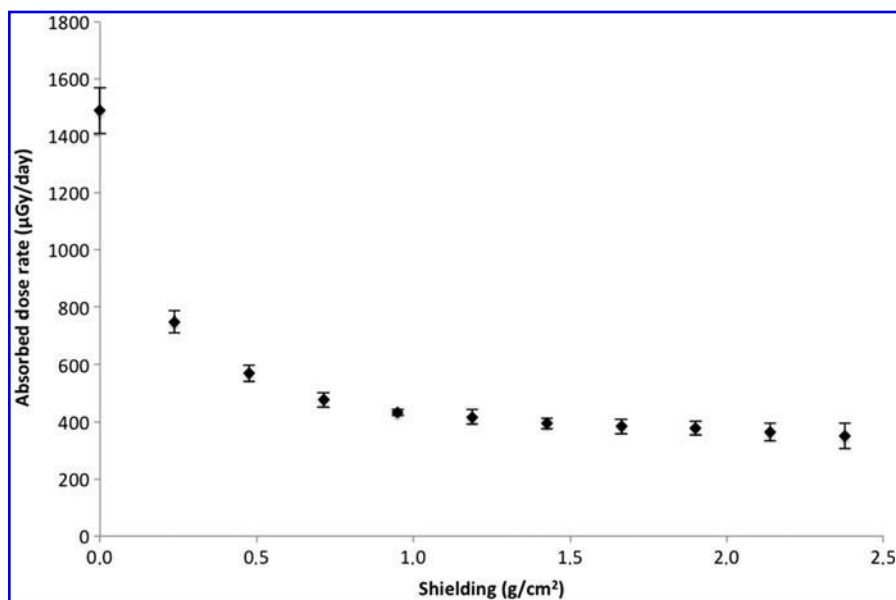
FIG. 5. Evolution of the absorbed dose rate as a function of the shielding. Measurements were performed on 5 stacks of 11 TLDs placed into the Tray 3 during EXPOSE-R2 mission. TLDs, thermoluminescent detectors.

long cycle, respectively. The aptamer S/Ref values were 23.3 ± 5.9, 23.5 ± 10.4, and 70.6 ± 20.8 for the reference, the 80°C peak, and long cycle, respectively. Consequently, there is no great impact of thermal variation upon the fluorescence properties of the freeze-dried dye. On the contrary, significant differences were observed with the 49merYm3′F aptamer, with the same order of S/Ref for the long cycle (70.6 ± 20.8) as for the reference of the free dye (74.5 ± 15.1). Both values are statistically identical ($p > 0.05$). One possible explanation could be that a long cycle affected the photochemical features of the fluorescein dye when attached to aptamer, and consequently induced both a decrease in the fluorescence anisotropy and a higher variability in all signals (Ruta *et al.*, 2009). Dye played a preponderant role in the performance of the FP assays (Perrier *et al.*, 2018).

K_d values of flight "upper and lower tray" samples are not statistically different from ground "DLR 5°C" and "CNES 5°C" controls. Consequently, based on the above considerations, our results showed that aptamer recognition abilities were not affected during the overall flight mission, or that the degradations are too small to be detected by our analysis protocol.

4. Conclusions

In recent years, we have used various facilities that produce protons, electrons, neutrons, and heavy ions to test whether cosmic particles could induce changes in aptamer-binding events. However, simulating the space radiation environment in Earth facilities remains impossible due to
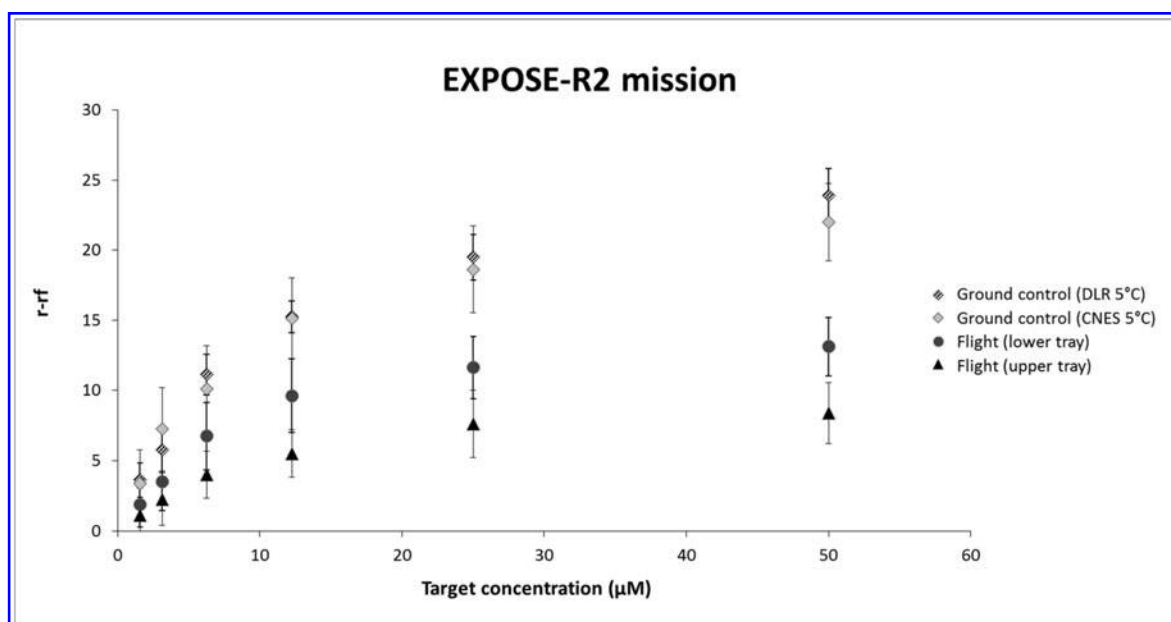

FIG. 6. Affinity curves for 49merYm3′F aptamer with additions of *L*-Tym obtained for controls and flight samples. The corresponding relative K_d values are given in Table 3. *L*-Tym, *L*-tyrosinamide.

the great number of variables. So, we also carried out a real space exposure of aptamer samples outside the ISS during the EXPOSE-R2 mission.

The results presented in this article suggest that cosmic radiation has no significant effect on the aptamers' recognition ability. On the contrary, repeated temperature cycling seems to alter the mobility of its fluorescein dye. This effect results in a lowering of the recognition step signal that could be interpreted as a loss of recognition, or as the absence of the target, or as an alteration of the fluorescent dye properties. In all cases, it alters the limit of detection of the biochip.

In our context, since we controlled the concentration of the target and we obtained K_d values similar to the reference value, we attribute the lowering of signal as a modification of fluorescent dye mobility. So, we suggest conducting further studies to improve the detection step by using another fluorescent dye or another detection method.

Acknowledgments

Author Disclosure Statement

No competing financial interests exist.

References

Baqué, M., Le Postollec, A., Coussot, G., Moreau, T., Desvignes, I., Incerti, S., Moretto, P., Dobrijevic, M., and Vandenabeele-Trambouze, O. (2011a) Biochip for astrobiological applications: investigation of low energy protons effects on antibody performances. *Planet Space Sci* 59:1490–1497.

Baqué, M., Le Postollec, A., Ravelet, C., Peyrin, E., Coussot, G., Desvignes, I., Incerti, S., Moretto, P., Dobrijevic, M., and Vandenabeele-Trambouze, O. (2011b) Investigation of low-energy proton effects on aptamer performance for astrobiological applications. *Astrobiology* 11:207–211.

Baqué, M., Dobrijevic, M., Le Postollec, A., Moreau, T., Faye, C., Vigier, F., Incerti, S., Coussot, G., Caron, J., and Vandenabeele-Trambouze, O. (2017) Irradiation effects on antibody performance in the frame of biochip-based instruments development for space exploration. *Int J Astrobiol* 16: 82–90.

Berger, T., Hajek, M., Bilski, P., Koerner, C., Vanhavere, F., and Reitz, G. (2012) Cosmic radiation exposure of biological test systems during the EXPOSE-E mission. *Astrobiology* 12:387–392.

Berger, T., Hajek, M., Bilski, P., and Reitz, G. (2015) Cosmic radiation exposure of biological test systems during the EXPOSE-R mission. *Int J Astrobiol* 14:27–32.

Cottin, H., Saiagh, K., Nguyen, D., Grand, N., Benilan, Y., Cloix, M., Coll, P., Gazeau, M.-C., Fray, N., Khalaf, D., Raulin, F., Stalport, F., Carrasco, N., Szopa, C., Chaput, D., Bertrand, M., Westall, F., Mattioda, A., Quinn, R., Ricco, A., Santos, O., Baratta, G., Strazzulla, G., Palumbo, M.E., Le

Postollec, A., Dobrijevic, M., Coussot, G., Vigier, F., Vandenabeele-Trambouze, O., Incerti, S., and Berger, T. (2015) Photochemical studies in low Earth orbit for organic compounds related to small bodies, Titan and Mars. Current and future facilities. *Bull Soc R Sci Liège* 84:60–73.

Cottin, H., Kotler, J.M., Billi, D., Cockell, C., Demets, R., Ehrenfreund, P., Elsaesser, A., d'Hendecourt, L., van Loon, J.J.W.A., Martins, Z., Onofri, S., Quinn, R.C., Rabbow, E., Rettberg, P., Ricco, A.J., Slenzka, K., de la Torre, R., de Vera, J.-P., Westall, F., Carrasco, N., Fresneau, A., Kawaguchi, Y., Kebukawa, Y., Nguyen, D., Poch, O., Saiagh, K., Stalport, F., Yamagishi, A., Yano, H., and Klamm, B.A. (2017) Space as a tool for astrobiology: review and recommendations for experimentations in earth orbit and beyond. *Space Sci Rev* 209:83–181.

Coussot, G., Moreau, T., Faye, C., Vigier, F., Baqué, M., Le Postollec, A., Incerti, S., Dobrijevic, M., and Vandenabeele-Trambouze, O. (2017) Biochip-based instruments development for space exploration: influence of the antibody immobilization process on the biochip resistance to freeze-drying, temperature shifts and cosmic radiations. *Int J Astrobiol* 16:190–199.

Coussot, G., Faye, C., Le Postollec, A., and Dobrijevic, M. (2018) A methodological approach for the thermal stability and stress exposure studies of a model antibody. *Anal Biochem* 548:23–31.

Coussot, G., Le Postollec, A., Faye, C., Baqué, M., Vandenabeele-Trambouze, O., Incerti, S., Vigier, F., Chaput, D., Cottin, H., Przybyla, B., Berger, T., and Dobrijevic, M. (2019) Photochemistry on the space station—antibody resistance to space conditions after exposure outside the International Space Station. *Astrobiology* 19:1053–1062.

de Diego-Castilla, G., Cruz-Gil, P., Mateo-Martí, E., Fernández-Calvo, P., Rivas, L.A., and Parro, V. (2011) Assessing antibody microarrays for space missions: effect of long-term storage, gamma radiation, and temperature shifts on printed and fluorescently labeled antibodies. *Astrobiology* 11:759–773.

Derveni, M., Hands, A., Allen, M., Sims, M.R., and Cullen, D.C. (2012) Effects of simulated space radiation on immunoassay components for life-detection experiments in planetary exploration missions. *Astrobiology* 12:718–729.

Derveni, M., Allen, M., Sawakuchi, G.O., Yukihara, E.G., Richter, L., Sims, M.R., and Cullen, D.C. (2013) Survivability of immunoassay reagents exposed to the space radiation environment on board the ESA BIOPAN-6 platform as a prelude to performing immunoassays on Mars. *Astrobiology* 13:93–102.

Dong, Y., Xu, Y., Yong, W., Chu, X., and Wang, D. (2014) Aptamer and its potential applications for food safety. *Crit Rev Food Sci Nutr* 54:1548–1561.

Gotrik, M.R., Feagin, T.A., Csordas, A.T., Nakamoto, M.A., and Soh, H.T. (2016) Analysis of aptamer discovery and technology. *Acc Chem Res* 49:1903–1910.

Hassler, D.M., Zeitlin, C., Wimmer-Schweingruber, R.F., Ehresmann, B., Rafkin, S., Eigenbrode, J.L., Brinza, D.E., Weigle, G., Böttcher, S., Böhm, E., Burmeister, S., Guo, J., Köhler, J., Martin, C., Reitz, G., Cucinotta, F.A., Kim, M.H., Grinspoon, D., Bullock, M.A., Posner, A., Gómez-Elvira, J., Vasavada, A., Grotzinger, J.P.; MSL Science Team; and Collaborators (438). (2014) Mars' surface radiation environment measured with the mars science laboratory's curiosity rover. *Science* 343:1244797.

Le Postollec, A., Dobrijevic, M., Incerti, S., Moretto, P., Seznec, H., Desorgher, L., Santin, G., Nieminen, P., Dartnell, L., Vandenabeele-Trambouze, O., and Coussot, G. (2007) Development of a biochip dedicated to planetary exploration. First step: resistance studies to space conditions. In *Journées*

Semaine de l'Astrophysique Française 2007, edited by J. Bouvier, A. Chalavaev, and C. Charbonnel, Société Française d'Astronomie et d'Astrophysique (SF2A), p 408.

Le Postollec, A., Coussot, G., Baqué, M., Incerti, S., Desvignes, I., Moretto, P., Dobrijevic, M., and Vandenabeele-Trambouze, O. (2009a) Investigation of neutron radiation effects on polyclonal antibodies (IgG) and fluorescein dye for astrobiological applications. *Astrobiology* 9:637–645.

Le Postollec, A., Incerti, S., Dobrijevic, M., Desorgher, L., Santin, G., Moretto, P., Vandenabeele-Trambouze, O., Coussot, G., Dartnell, L., and Nieminen, P. (2009b) Monte Carlo simulation of the radiation environment encountered by a biochip during a space mission to Mars. *Astrobiology* 9:311–323.

Martins, Z. (2011) In situ biomarkers and the life marker chip. *Astron Geophys* 52:1.34–1.35.

McKay, C.P., Stoker, C.R., Glass, B.J., Davé, A., Davila, A.F., Heldmann, J.L., Marinova, M.M., Fairen, A.G., Quinn, R.C., Zacny, K.A., Paulsen, G., Smith, P.H., Parro, V., Andersen, D.T., Hecht, M.H., Lacelle, D., and Pollard, W.H. (2013) The icebreaker life mission to mars: a search for biomolecular evidence for life. *Astrobiology* 13:334–353.

Parro, V., Rodriguez-Manfredi, J.A., Briones, C., Compostizo, C., Herrero, P.L., Vezb, E., Sebastián, E., Moreno-Paz, M., García-Villadangos, M., Fernández-Calvo, P., González-Toril, E., Pérez-Mercader, J., Fernández-Remolar, D., and Gómez-Elvira, J. (2005) Instrument development to search for biomarkers on mars: terrestrial acidophile, iron-powered chemolithoautotrophic communities as model systems. *Planet Space Sci* 53: 729–737.

Parro, V., Fernández-Remolar, D., Rodríguez-Manfredi, J.A., Cruz-Gil, P., and Gómez-Elvira, J. (2008) SOLID2: an antibody array-based Life-detector instrument in a Mars drilling simulation experiment (MARTE). *Astrobiology* 8:987–999.

Parro, V., de Diego-Castilla, G., Rodríguez-Manfredi, J.A., Rivas, L.A., Blanco-López, Y., Sebastián, E., Romeral, J., Compostizo, C., Herrero, P.L., García-Marín, A., Moreno-Paz, M., García-Villadangos, M., Cruz-Gil, P., Peinado, V., Martín-Soler, J., Pérez-Mercader, J., and Gómez-Elvira, J. (2011a) SOLID3: a multiplex antibody microarray-based optical sensor instrument for in situ life detection in planetary exploration. *Astrobiology* 11:15–28.

Parro, V., Fernández-Remolar, D., Rodríguez-Manfredi, J.A., Cruz-Gil, P., Rivas, L.A., Ruiz-Bermejo, M., Moreno-Paz, M., García-Villadangos, M., Gómez-Ortiz, D., Blanco-López, Y., Menor-Salván, C., Prieto-Ballesteros, and O., Gómez-Elvira, J. (2011b) Classification of modern and Old Rio Tinto sedimentary deposits through the biomolecular record using a Life Marker Biochip: implications for detecting life on Mars. *Astrobiology* 11:29–44.

Perrier, S., Ravelet, C., Guieu, V., Roy, B., Perigaud, C., and Peyrin, E. (2010) Rationally designed aptamer-based fluorescence polarization sensor dedicated to the small target analysis. *Biosens Bioelectron* 25:1652–1657.

Perrier, S., Guieu, V., Chovelon, B., Ravelet, C., and Peyrin, E. (2018) Panoply of fluorescence polarization/anisotropy signaling mechanisms for functional nucleic acid-based sensing platforms. *Anal Chem* 90:4236–4248.

Rabbow, E., Rettberg, P., Parpart, A., Panitz, C., Schulte, W., Molter, F., and Willnecker, R. (2017) EXPOSE-R2: the astrobiological ESA mission on board of the international space station. *Front Microbiol* 8:1533.

Rozenblum, G.T., Lopez, V.G., Vitullo, A.D., and Radrizzani, M. (2016) Aptamers: current challenges and future prospects. *Expert Opin Drug Discovery* 11:127–135.

Ruta, J., Perrier, S., Ravelet, C., Fize, J., and Peyrin, E. (2009) Noncompetitive fluorescence polarization aptamer-based assay for small molecule detection. *Anal Chem* 81:7468–7473.

Sims, M.R., Pullan, D., Holt, J., Blake, O., Sykes, J., Samara-Ratna, P., Canali, M., Cullen, D.C., Rix, C.S., Buckley, A., Derveni, M., Evans, D., Miguel García-Con, L., Rhodes, A., Rato, C.C., Stefinovic, M., Sephton, M.A., Court, R.W., Bulloch, C., Kitchingman, I., Ali, Z., Borst, G., Leeuwis, H., Prak, A., Norfini, A., Geraci, E., Tavanti, M., Brucato, J., and Holm, N. (2012) Development status of the life marker chip instrument for ExoMars. *Planet Space Sci* 72:129–137.

Smith, H. and Parro, V. (2014) Planetary protection plan for an antibody based instrument proposed for Mars2020. In *40th COSPAR Scientific Assembly*. p 3140.

Song, K.-M., Lee, S., and Ban, C. (2012) Aptamers and their biological applications. *Sensors (Basel)* 12:612–631.

Vigier, F., Le Postollec, A., Coussot, G., Chaput, D., Cottin, H., Berger, T., Triqueneaux, S., Dobrijevic, M., and Vandenabeele-Trambouze, O. (2013) Preparation of the biochip experiment on the EXPOSE-R2 mission outside the International Station. *Adv Space Res* 52:2168–2179.

Zhu, Z., Schmidt, T., Mahrous, M., Guieu, V., Perrier, S., Ravelet, C., and Peyrin, E. (2011) Optimization of the structure-switching aptamer-based fluorescence polarization assay for the sensitive tyrosinamide sensing. *Anal Chim Acta* 707:191–196.

Address correspondence to:
Gaëlle Coussot
ENSCM
CNRS
Université de Montpellier
Institut des Biomolécules Max Mousseron (IBMM)
Montpellier 34093 Cedex 5
France

E-mail: gaelle.coussot@umontpellier.fr

Abbreviations Used

FP = fluorescence polarization
GCR = galactic cosmic radiation
ISS = International Space Station
L-Tym = L-tyrosinamide
MUSC = Microgravity User Support Center
MW = molecular weight
NHS = N-hydroxysuccinimide modified surface
PSS = Photochemistry on the Space Station
RH = relative humidity
RFN = Response of the Fluorescence Noise
RFS = Response of the Fluorescence Signal
SEP = solar energetic particles
TLDs = thermoluminescent detectors

This article has been cited by:

1. Cottin Hervé, Rettberg Petra. 2019. EXPOSE-R2 on the International Space Station (2014–2016): Results from the PSS and BOSS Astrobiology Experiments. *Astrobiology* **19**:8, 975-978. [Abstract] [Full Text] [PDF] [PDF Plus]

2. Coussot Gaëlle, Le Postollec Aurélie, Faye Clément, Baqué Mickaël, Vandenabeele-Trambouze Odile, Incerti Sébastien, Vigier Flavie, Chaput Didier, Cottin Hervé, Przybyla Bartos, Berger Thomas, Dobrijevic Michel. 2019. Photochemistry on the Space Station—Antibody Resistance to Space Conditions after Exposure Outside the International Space Station. *Astrobiology* **19**:8, 1053-1062. [Abstract] [Full Text] [PDF] [PDF Plus]